Date December 2008
Author Serge L. Toxopeus
Address Delft University of Technology
Ship Hydromechanics Laboratory
Mekelweg 2, 26282 CD Delft

TUDelft

Delft University of Technology

Deriving mathematical manoeuvring models for bare ship hulls using viscous flow calculations

by

Serge L. Toxopeus

Report No. 1603-P 2008

Published in: Journal of Marine Science and Technology, Volume 13, Nr. 4, Publ. Springer Japan, ISSN 0948-4280

SpringerLink

Content Types **Subject Collections**

Back to: Journal

Journal

Institutional Login

Recognized as:

Technische Universiteit Delft (150-40-965)

1034 UKB (593-67-639)

1254 UKB Netherlands Landolt Börnstein (577-14-382)

1260 UKB Netherlands LNCS incl. archives (592-86-894)

1261 UKB Netherlands LNP (445-61-068)

1262 UKB Netherlands LNCIS (768-53-520)

1263 UKB Netherlands LNM (191-45-973)

UKB Netherlands (add. 119 titels) (470-19-176)

UKB Netherlands Brill (711-55-095)

UKB Netherlands LNES (617-63-136)

UKB Netherlands OJA (957-05-043)

UKB Netherlands OJA (2) (127-79-678)

Welcome!

To use the personalized features of this site, please **log in** or **register**.

If you have forgotten your username or password, we can **help**.

My Menu

Marked Items

Alerts

Order History

Saved Items

All

Favorites

Journal of Marine Science and Technology

Publisher	Springer Japan
ISSN	0948-4280 (Print) 1437-8213 (Online)
Subject Collection	Engineering
Subject	Engineering, Automotive and Aerospace Engineering, Traffic, Engineering Fluid Dynamics, Engineering Design, Offshore Engineering and Mechanical Engineering
SpringerLink Date	Friday, April 05, 2002

the language of science

Editorial View | Condensed List View | Expanded List View

13 Volumes

First | **Current-7** | 6-1 | Next

J Mar Sci Technol
DOI 10.1007/s00773-008-0002-9

ORIGINAL ARTICLE

Deriving mathematical manoeuvring models for bare ship hulls using viscous flow calculations

Serge L. Toxopeus

Received: 13 June 2007 / Accepted: 29 November 2007

Abstract To assess the manoeuvrability of ships at the early design stage, reliable simulation models are required. Traditionally, these tools have used empiric descriptions of the forces and moments on the ship's hull. However, nowadays new computational techniques are available enabling more reliable predictions of the manoeuvring behaviour of ships. In this article, a mathematical manoeuvring model to predict the forces and moments on a bare ship hull is presented. Special attention is paid to application in simulators in which also astern or sideways manoeuvring should be possible. The hydrodynamic derivatives in this model were determined by a hybrid approach using results of viscous flow calculations supplemented by semi-empirical methods. It was demonstrated that this approach leads to a considerable improvement in the prediction of the forces and moments on the ship compared to using conventional empiric derivatives published in the literature.

Keywords CFD · RANS · Viscous flow · Ship manoeuvring · Mathematical model

This work was presented in part at the International Conference on Computational Methods in Marine Engineering—MARINE 2007, Barcelona, June 3–4, 2007.

S. L. Toxopeus (✉)
Maritime Research Institute Netherlands/Delft University of Technology,
P.O. Box 28, 6700 AA Wageningen,
The Netherlands
e-mail: S.L.Toxopeus@MARIN.NL

1 Introduction

To assess the manoeuvrability of ships at the early design stage, reliable simulation models are required. Traditionally, simulations have focused on assessing compliance with the manoeuvring standards set by the International Maritime Organisation (IMO) [1]. However, due to emerging owner or operational requirements, the need has arisen for assessment of manoeuvring capabilities in operations other than the manoeuvring conditions prescribed by the IMO requirements, see, for example, Quadvlieg and Van Coevorden [2] or Dand [3].

The traditional tools use empiric descriptions of the forces and moments on the ship's hull and are generally based on regression analysis of captive manoeuvring test data for a (preferably wide) range of ships. Due to the lack of resolution of hull details or application outside the range of the regression database, the prediction of the manoeuvrability may be unreliable. Therefore, new methods are required to obtain reliable and accurate manoeuvring simulation models. These methods should not only be suitable to predict the yaw checking and turning ability of the ship according to the IMO requirements, but also be applicable to operation in confined waterways or harbour manoeuvring assessment studies, for example.

In the present article, the work conducted by the author regarding efficient determination of hydrodynamic coefficients for manoeuvring ships within the manoeuvring work package of the EU Virtual Towing Tank Utility in Europe (VIRTUE) project is presented. Based on various viscous flow calculations for steady drift motion, steady yaw motion, and combined drift/yaw motion (similar work can be found in Cura Hochbaum and Vogt [4] or Ohmori [5]), a mathematical model for the bare hull forces and moments is derived. This process mimics the approach taken when using computerized planar motion carriage (CPMC), planar motion mechanism (PMM), or rotating arm experiments to generate a mathematical model and is sometimes referred to as virtual CPMC/PMM or a virtual towing tank.

Comparisons with experimental data obtained within the project show that using accurate viscous flow calculations, a considerable improvement in the prediction of the forces and moments on ships can be obtained compared to conventional empirical methods.

1.1 Test cases

Three hull forms were considered in this study. The first ship was the Hamburg Test Case (HTC), a single-screw container vessel; the second ship was the Maritime Research Institute Netherlands (MARIN) liquefied natural gas (LNG) carrier with twin gondolas, see also Jürgens et al. [6] and the third ship was a modified version of the Korean Research Institute of Ships and Ocean Engineering (KRISO) Very Large Crude Carrier (VLCC) 2, designated KVLCC2M, which was one of the subjects of the Tokyo Computational Fluid Dynamics (CFD) Workshop [7]. The main particulars of these ships are presented in Table 1 and the body plans can be found in Fig. 1.

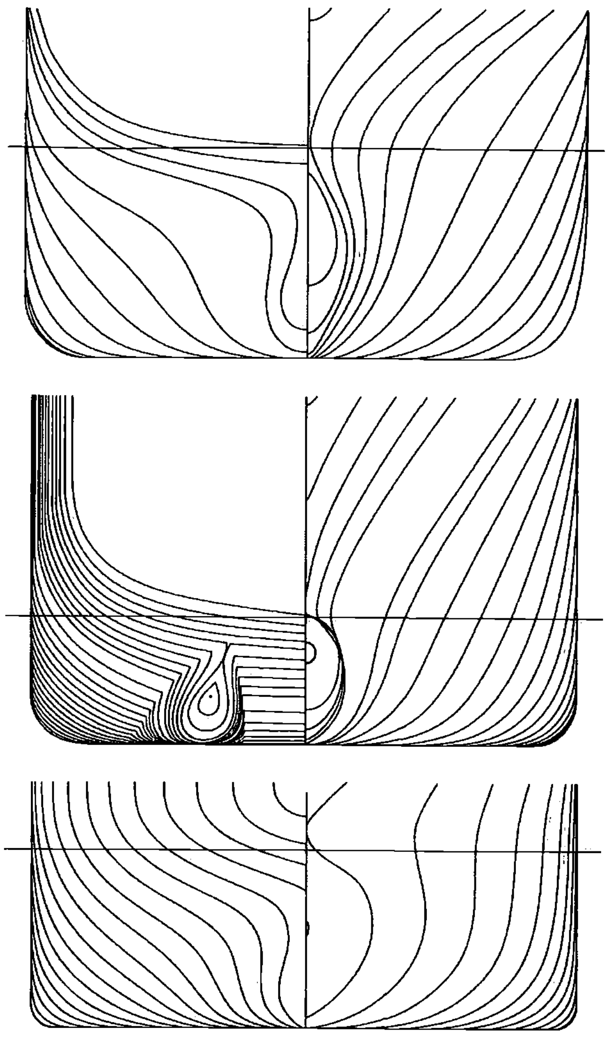

Fig. 1 Body plans of the ships: *top* Hamburg Test Case (HTC); *middle*, Maritime Research Institute Netherlands liquefied natural gas carrier (MARIN LNG); *bottom*, modified Korean Research Institute of Ships and Ocean Engineering Very Large Crude Carrier 2 (KVLCC2M)

2 Numerical procedures

2.1 Flow solver, turbulence model, and computational domain

All calculations were performed with the MARIN in-house flow solver PARNASSOS, which is based on a finite-difference discretization of the Reynolds-averaged continuity and momentum equations, using fully collocated variables and discretization. The equations are solved with a coupled procedure, retaining the continuity equation in its original form. The governing equations are integrated down to the wall, that is, no wall functions are used. More detailed information about the solver can be found in Hoekstra [8] or Raven et al. [9]. For all calculations, the one-equation turbulence model proposed by Menter [10] was used. The Spalart correction (see [11]) of the stream-wise vorticity was included.

The results presented in this article were all obtained on structured grids with H-O topology, using grid clustering near the bow and propeller plane. Appendages were not present during the tests and therefore were not modelled in the calculations. The calculations were conducted without incorporating free-surface deformation. Based on the speeds used during the tests for these ships and the range of drift angles studied, the effects of speed and free-surface

Table 1 Main particulars of the test cases

Description	Symbol	HTC	MARIN LNG	KVLCC2M
Length between perpendiculars (m)	L_{pp}	153.7	300	320
Length/beam ratio	L_{pp}/B	5.59	6.00	5.52
Length/draught ratio	L_{pp}/T	14.92	25.64	15.38
Beam/draught ratio	B/T	2.67	4.27	2.79
Block coefficient	C_b	0.65	0.73	0.81
Scale ratio	λ	24	43.158	64.386

HTC Hamburg test case, *MARIN LNG* Maritime Research Institute Netherlands liquefied natural gas carrier, *KVLCC2M* modified Korean Research Institute of Ships and Ocean Engineering Very Large Crude Carrier 2 deformation on the forces on the manoeuvring ship are likely to be small.

For the zero drift cases, a single-block calculation was conducted, whereas for non-zero drift, the domain was effectively decomposed into two blocks. The six boundaries of the computational domain were as follows: the inlet boundary was a transverse plane located upstream of the forward perpendicular; the outlet boundary was a transverse plane downstream of the aft perpendicular; the external boundary was a circular or elliptical cylinder for the drift cases and doughnut shaped for the rotation or combined motion cases; the remaining boundaries were the ship surface, the symmetry plane of the ship or coinciding block boundaries, and the undisturbed water surface.

The flow around the hull at non-zero drift angles has no port-starboard symmetry and the computational domain must be extended to cover the port side as well. Furthermore, a larger domain is required in order to incorporate the drift angle. On each side of the domain, the grid consisted of an inner block and an outer block, see Fig. 2. The inner block was the same for all calculations and the outer block could deform to allow for the drift angle, the rotational motion of the ship, or both. Therefore, grids for various manoeuvring motions could be made efficiently. Use was made of an in-house grid generator, see Eça et al. [12].

2.2 Coordinate system and non-dimensionalization

The origin of the right-handed system of axes used in this study for the forces and moments was located at the intersection of the water plane, midship, and the centre plane, with the longitudinal force X directed forward, the transverse force Y to starboard, and Z vertically downward.

A positive drift angle β corresponds to the flow coming from the port side [i.e., $\beta = \arctan(-v/u)$], with u the longitudinal ship velocity component and v the transverse ship velocity component. A positive non-dimensional yaw rate γ corresponds to the bow turning to starboard and is defined as $\gamma = r\ L_{pp}/V_s$, where r is the yaw rate, L_{pp} is the length between perpendiculars, and V_s is the speed of the ship.

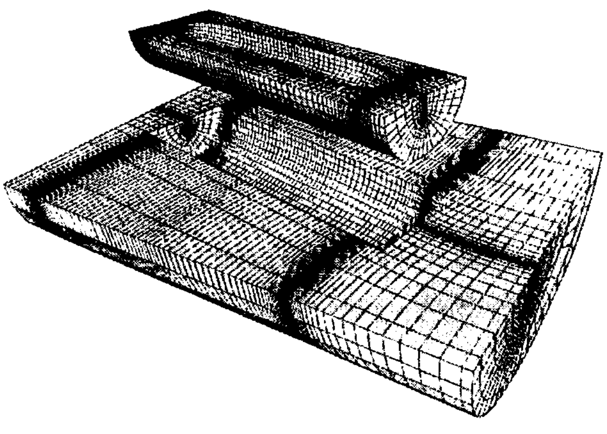

Fig. 2 Impression of inner and outer blocks (coarsened for presentation) for the drift angle case

All forces and moments were presented non-dimensionally. The longitudinal force X and transverse force Y were made non-dimensional using $\frac{1}{2}\rho V_s L_{pp} T$ and the yaw moment N by $\frac{1}{2}\rho V_s L_{pp}^2 T$, where ρ is the density of water, and T is the draught.

3 Calculations

Series of calculations were carried out to derive the required hydrodynamic coefficients. In Tables 2 and 3, overviews are given of the calculations that were conducted and the corresponding grid sizes, respectively. The results of the calculations using these grids were used to derive the coefficients for the mathematical model that is presented below.

In Toxopeus [13, 14] more information can be found about the calculations and sensitivity studies conducted for the KVLCC2M and HTC, respectively. Summarizing, the uncertainty due to discretization errors in the transverse force Y was found to be below 9% and the uncertainty in the yawing moment was found to be below 15% (including safety factors of 1.25 and 3, respectively).

3.1 Mathematical manoeuvring model

When setting up a mathematical model to describe the forces on a ship due to manoeuvring motion, the intended use of the model determines the structure of the model itself. For example, when simulator studies incorporating harbour manoeuvres are to be conducted, the model should be able to accurately describe the forces and moments on the ship during transverse motions, turning on the spot, and sailing astern. In the present work, it is assumed that the manoeuvring model should be valid for a wide range of applications, including low-speed and harbour manoeuvres. Presently, only viscous flow calculations have been conducted for the bare hull, and therefore attention is focused on the description of the forces and moments on the bare hull only. The influence of other components such as propellers and rudders will be incorporated in future work.

Mathematical manoeuvring models for the bare hull consist, in general, of three different components: (added) mass coefficients, damping coefficients, and spring coefficients. In earlier work by Vassalos et al. [15], Ishiguro et al. [16] and Lee and Shin [17], for example, or more recently, Bulian et al. [18] it was found that the sensitivity of the manoeuvrability to changes in the added mass coefficients is small. Therefore, it is assumed that the added mass

Table 2 Overview of the calculations

Series	HTC	MARIN LNG	KVLCC2M
Experiment (Fn)	0.132	0.185	0.142
Calculation (Re)	6.3×10^6	9.2×10^6	3.945×10^6
Pure drift, β	0°, 2.5°, 5°, 10°, 15°	0°, 2.5°, 5°, 10°, 20°, 30°	0°, 3°, 6°, 9°, 12°, 15°, 18°
Pure yaw, γ	0.1, 0.15, 0.2, 0.3, 0.4, 0.556	–	0.1, 0.2, 0.25, 0.3, 0.4, 0.6
Combined motion (β, γ)	(5°, 0.2), (10°, 0.2), (6°, 0.4), (10°, 0.4), (15°, 0.4)	–	(12°, 0.1), (12°, 0.3), (12°, 0.6)

In the calculations, free-surface deformation was neglected

The Reynolds number (*Re*) used for the calculations was based on the speed used during the experiments

Fn Froude number

Table 3 Number of grid nodes used in the calculations in the longitudinal, wall-normal, and girthwise directions

Series	HTC	MARIN LNG	KVLCC2M
Pure drift	$377 \times 95 \times 51 \times 2 = 3.7 \times 10^6$	$321 \times 73 \times 85 = 2.0 \times 10^6$ ($\beta = 0$) $161 \times 54 \times 44 \times 2 = 7.7 \times 10^5$ ($\beta = 10$) $107 \times 36 \times 30 \times 2 = 2.3 \times 10^5$ ($\beta \neq 0$, $\beta \neq 10$)	$449 \times 95 \times 45 \times 2 = 3.8 \times 10^6$
Pure yaw	$297 \times 77 \times 82 = 3.1 \times 10^6$ ($\gamma < 0.3$)	–	$257 \times 55 \times 23 \times 2 = 6.5 \times 10^5$ ($\gamma < 0.3$)
	$257 \times 65 \times 70 = 1.2 \times 10^6$ ($\gamma \geq 0.3$)		$129 \times 28 \times 12 \times 2 = 8.7 \times 10^4$ ($\gamma \geq 0.3$)
Combined motion	$257 \times 65 \times 70 = 1.2 \times 10^6$	–	$129 \times 28 \times 12 \times 2 = 8.7 \times 10^4$

coefficients can be approximated reliably by using empiric formulas such as, for example, those published by Clarke et al. [19] or Hooft and Pieffers [20]. Due to this assumption, no calculations are required to obtain the added mass coefficients. When only horizontal manoeuvres are considered, and neglecting the heel angle, spring coefficients do not have to be taken into account.

The following non-dimensionalized (indicated by a prime in the equations below) mathematical model for the longitudinal force X, transverse force Y, and yawing moment N is adopted:

$$X' = X'_{u|u|} \cdot \cos\beta \cdot |\cos\beta| + X'_{\beta\gamma} \cdot \cos\beta \cdot \gamma \tag{1}$$

$$\begin{aligned} Y' = {} & Y'_{\beta} \cdot |\cos\beta| \cdot \sin\beta + Y'_{\gamma} \cdot \cos\beta \cdot \gamma + Y'_{\beta|\beta|} \cdot \sin\beta \cdot |\sin\beta| \\ & + Y'_{\beta|\gamma|} \cdot \beta|\gamma| + Y'_{ab} \cdot \left|\cos^{a_y}\beta \cdot \sin^{b_y}\beta\right| \cdot \operatorname{sign}\sin\beta \end{aligned} \tag{2}$$

$$\begin{aligned} N' = {} & N'_{\beta} \cdot \cos\beta \cdot \sin\beta + N'_{\gamma} \cdot |\cos\beta| \cdot \gamma \\ & + N'_{u\gamma c} \cdot |\cos\beta \cdot \gamma^{c_n}| \cdot \operatorname{sign}\gamma + N'_{\gamma|\gamma|} \cdot \gamma \cdot |\gamma| \\ & + \left(N'_{\beta\beta\gamma} \cdot \beta + N'_{\beta\gamma\gamma} \cdot \gamma \cdot \operatorname{sign}\cos\beta\right) \cdot \beta\gamma \\ & + N'_{ab} \cdot \left|\cos^{a_n}\beta \cdot \sin^{b_n}\beta\right| \cdot \operatorname{sign}(\cos\beta \cdot \sin\beta) \end{aligned} \tag{3}$$

where a_y, b_y, a_n, b_n and c_n are integer constants determined during the curve fitting. At zero speed, the non-dimensional yaw rate γ, and subsequently the non-dimensional $N'_{\gamma|\gamma|}$ contribution, will become infinite and therefore due care has to be taken when implementing this mathematical model in a simulation program. This problem can be solved by using the $N'_{\gamma|\gamma|}$ term in a fully dimensional form.

The damping coefficients in the mathematical model are derived in four steps:

1. The linear coefficients for simple motions (slope of force or moment curves at $\beta = 0$ resp. $\gamma = 0$) are found as follows. For steady drift manoeuvres, the obtained forces or moments are divided by $\cos\beta \cdot \sin\beta$ and the coefficients are taken from the intersection at $\beta = 0°$ of a linear or polynomial trend line through the data points. For steady rotation, the same procedure is applied on the forces and moments divided by γ.
2. Non-linear coefficients for pure transverse motion ($\beta = 90°$) and pure rotation ($V = 0$) are found using empirical relations (based on the work of Hooft [21], e.g.). Currently, due to the unsteady nature of these manoeuvres, these motions are not solved using viscous flow calculations.
3. Other non-linear components for simple motions can be determined by subtracting the contributions from the coefficients found in steps 1 and 2 from the calculated total bare hull forces; the non-linear components for the simple motions can then be determined using curve fitting.

4. The cross-terms, based on combined motions, are found in a similar way to step 3. The known contributions of the coefficients from steps 1–3 are subtracted from the calculated bare hull forces and the remainder is used to fit the cross-terms.

This approach is chosen to enable accurate modelling of the linearized behaviour for course-keeping (step 1), realistic modelling of the harbour manoeuvring characteristics (step 2), and accurate modelling of non-linear manoeuvres (steps 3 and 4). To ensure appropriate responses for astern manoeuvres, it is assumed that the forces and moments on the hull during astern manoeuvres are identical to those during ahead manoeuvring. If different forces and moments are desired for astern motion, this can be achieved by selecting the linear derivatives based on the sign of the longitudinal ship velocity, for example, as follows for the coefficient Y'_{β}, with $Y'_{\beta,\mathrm{ahead}}$ the appropriate coefficient for ahead speed and $Y'_{\beta,\mathrm{astern}}$ for astern speed:

$$Y'_{\beta} = Y'_{\beta,\mathrm{ahead}} \cdot \max(0, \mathrm{sign}(\cos\beta)) + Y'_{\beta,\mathrm{astern}} \cdot \max(0, -\mathrm{sign}(\cos\beta)) \tag{4}$$

With Eqs. 1–3 as the mathematical formulation for the bare hull manoeuvring forces, the hydrodynamic derivatives are determined using the results of the available viscous flow calculations presented in Table 2. Table 4 shows the obtained manoeuvring coefficients.

In Figs. 3, 4 and 5, the correspondence of the calculations and the predicted forces and moments (based on the mathematical model) with the measurements is graphically presented. Figure 6 shows the results of the mathematical model for combined motion compared to the results obtained by the viscous flow calculations. The experimental values for the HTC and MARIN LNG carrier were obtained by Hamburgische Schiffbau-Versuchanstalt

Table 4 Estimated bare hull manoeuvring coefficients

Step	Coefficient	HTC	MARIN LNG	KVLCC2M
1	Y'_{β}	0.1830	0.0416	0.1166
	Y'_{γ}	0.0250	–	0.0475
2	$Y'_{\beta\lvert\beta\rvert}$	1.1100	0.9662	0.9788
3	Y'_{ab}	−0.6552	−0.9802	−0.5955
	a_y	3	2	2
	b_y	2	3	3
4	$Y'_{\beta\lvert\gamma\rvert}$	0.1635	–	0.2645
1	N'_{β}	0.1403	0.0894	0.1530
	N'_{γ}	−0.0270	–	−0.0251
2	$N'_{\gamma\lvert\gamma\rvert}$	−0.0375	−0.0351	−0.0299
3	N'_{ab}	0.1314	−0.0373	−0.0289
	a_n	1	3	4
	b_n	3	2	1
	$N'_{u\gamma c}$	−0.0073	–	0.0160
	c_n	2	–	3
4	$N'_{\beta\beta\gamma}$	−0.8682	–	−0.0765
	$N'_{\beta\gamma\gamma}$	0.2753	–	−0.0880

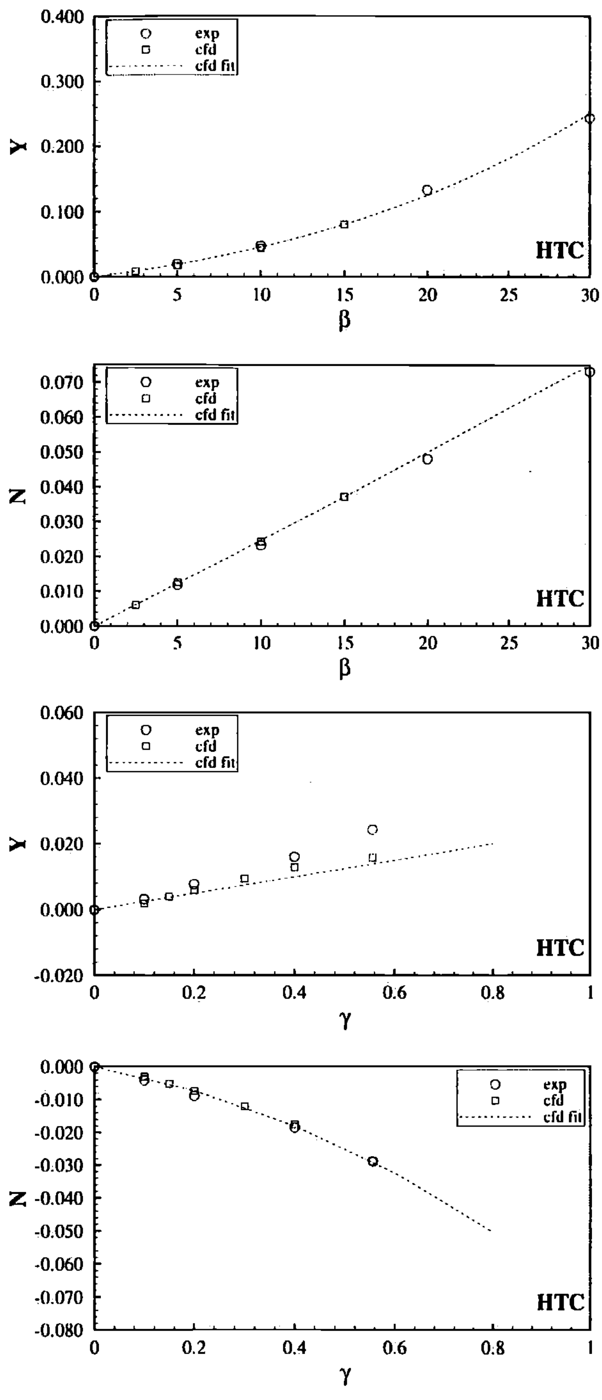

Fig. 3 Comparison between experiments and predicted forces and moments for HTC. *Y* transverse force, *N* yaw moment, γ yaw rate, *exp* experimental results, *cfd* results based on the viscous flow calculations, *cfd fit* results based on the mathematical model

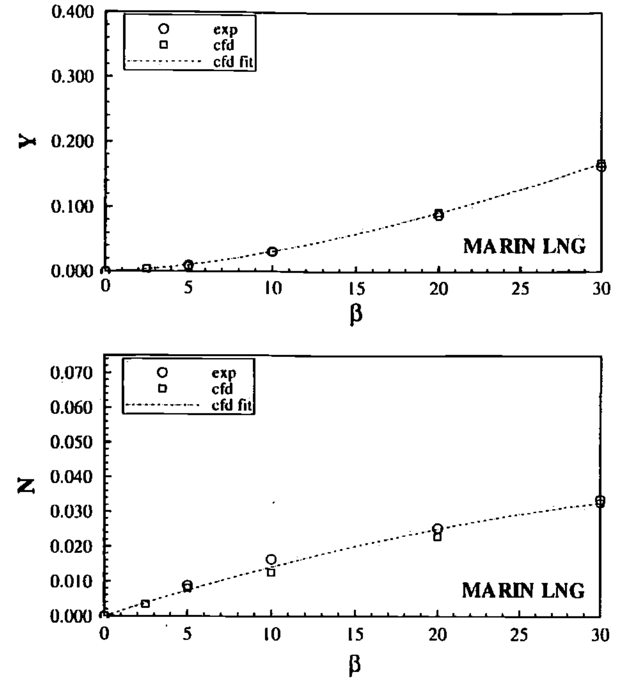

Fig. 4 Comparison between experiments and predicted forces and moments for MARIN LNG. β drift angle

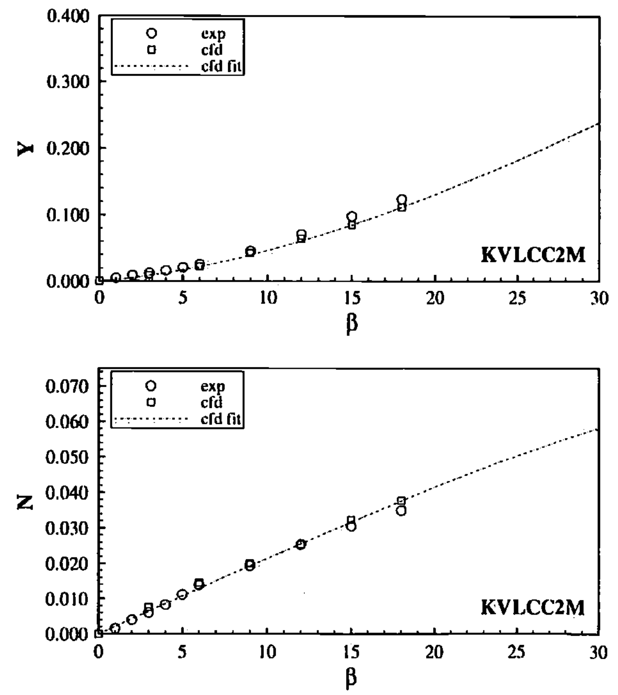

Fig. 5 Comparison between experiments and predicted forces and moments for KVLCC2M

(HSVA) within the VIRTUE project. The KVLCC2M experiments were conducted by National Maritime Research Institute (NMRI) [7, 22].

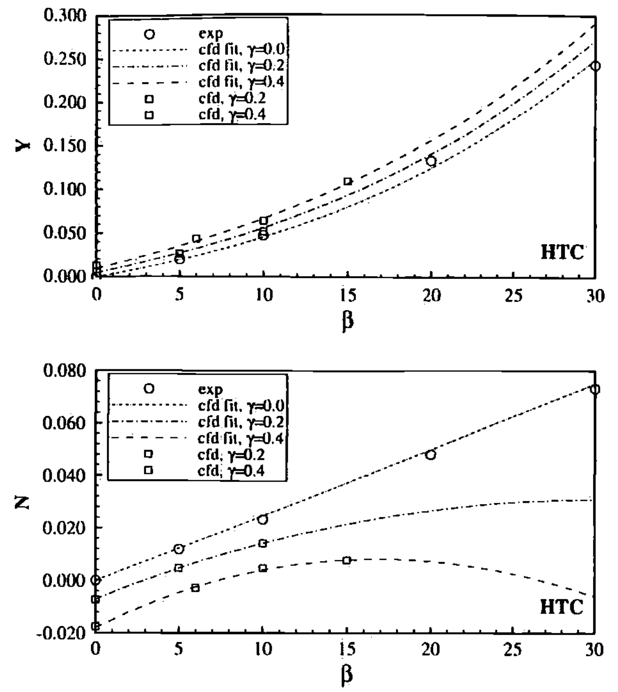

Fig. 6 Predicted forces and moments for combined motion for HTC

Table 5 Comparison of linear coefficients, HTC

Method	Y'_β	N'_β	$\frac{N'_\beta}{Y'_\beta}$	Y'_γ	N'_γ	$\frac{N'_\gamma}{Y'_\gamma - m'}$
Kijima [23]	0.373	0.134	0.359	0.158	−0.054	0.730
Vassalos [15]	0.373	0.110	0.294	0.067	−0.053	0.323
Clarke [19]	0.357	0.139	0.390	0.067	−0.053	0.323
Norrbin [19]	0.365	0.130	0.356	0.092	−0.078	0.553
exp	0.175	0.137	0.782	0.032	−0.039	0.192
cfd	0.183	0.140	0.767	0.025	−0.027	0.130
sb [24]	0.253	0.151	0.598	0.058	−0.038	0.215

exp Experimental results, *cfd* results based on viscous flow calculations, *sb* results based on the slender body theory

Good agreement with the experiments (exp) is seen for the results based on the viscous flow calculations (cfd) and based on the mathematical model (cfd-fit). Only the HTC results for the transverse force Y for pure yaw (γ) deviate from the measured results. The magnitude of the Y force during pure rotation is, however, very small and is of less significance than the other force or moment components.

Although the flow fields around the three ships are completely different, the present study demonstrates that for these ships, good predictions of the manoeuvring forces are obtained when using an accurate viscous flow solver.

Table 6 Comparison of linear coefficients, MARIN LNG

Method	Y'_β	N'_β	$\frac{N'_\beta}{Y'_\beta}$	Y'_γ	N'_γ	$\frac{N'_\gamma}{Y'_\gamma - m'}$
Kijima [23]	0.293	0.078	0.266	0.137	−0.036	0.338
Vassalos [15]	0.265	0.095	0.359	0.058	−0.040	0.213
Clarke [19]	0.276	0.073	0.264	0.058	−0.040	0.213
Norrbin [19]	0.217	0.074	0.339	0.033	−0.036	0.168
exp	0.058	0.105	1.812	0.025	−0.025	0.112
cfd	0.042	0.089	2.151	–	–	–
sb [24]	0.127	0.119	0.933	0.061	−0.010	0.055

Table 7 Comparison of linear coefficients, KVLCC2M

Method	Y'_β	N'_β	$\frac{N'_\beta}{Y'_\beta}$	Y'_γ	N'_γ	$\frac{N'_\gamma}{Y'_\gamma - m'}$
Kijima [23]	0.410	0.130	0.317	0.195	−0.053	0.540
Vassalos [15]	0.368	0.075	0.204	0.066	−0.053	0.231
Clarke [19]	0.389	0.134	0.345	0.066	−0.053	0.231
Norrbin [19]	0.357	0.125	0.350	0.076	−0.070	0.319
exp	0.166	0.140	0.844	–	–	–
cfd	0.117	0.153	1.312	0.047	−0.025	0.102
sb [24]	0.260	0.180	0.691	0.073	−0.051	0.232

3.2 Comparison with empirical and semi-empirical methods

In the literature, several researchers have published empirical formulas to estimate the linear manoeuvring derivatives, see Clarke et al. [19], Vassalos et al. [15] and Kijima et al. [23], for example. In Tables 5, 6 and 7, the derivatives based on the main particulars of the HTC, MARIN LNG, and KVLCC2M, respectively, are given according to these publications. Furthermore, the derivatives based on the measurements (exp), on the viscous flow calculations (cfd), and on the slender-body theory (sb, see [24], e.g.) are presented. The deviations ε of the predictions from the experimental values are shown in Fig. 7. The deviation is defined as $\varepsilon = (\text{prediction/experiment} - 1) \times 100\%$.

It is seen that, in general, both the viscous flow calculations and the slender-body coefficients approximate the experimental values better than the other empiric formulas. In particular, the destabilizing (N'_β/Y'_β) and stabilizing ($N'_\gamma/(Y'_\gamma - m')$) arms more accurately reflect the experimental values. The deviations from the experimental results show the drawback of empirical methods compared to semi-empirical methods or using viscous flow calculation results: during the derivation of the empirical formulas, a fixed database of ships is used. Depending on the types of ships in the database and the ship upon which the method is to be applied, accurate or inaccurate predictions of the forces and moments can be obtained.

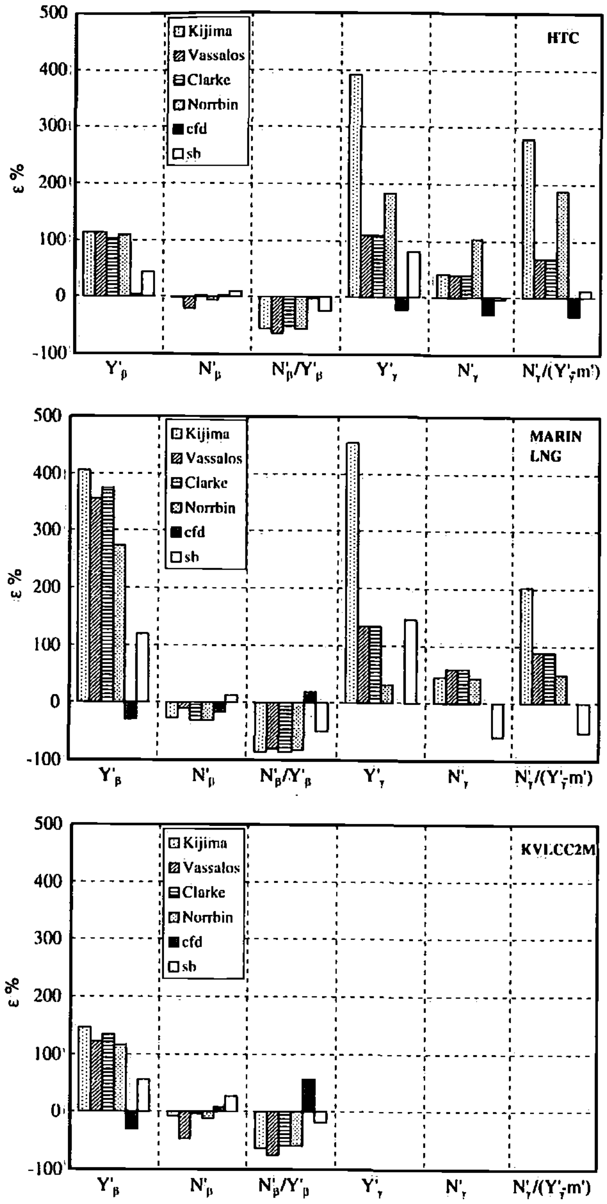

Fig. 7 Comparison of errors in prediction of linear coefficients. *sb* slender body theory

3.3 Sensitivity study

In order to determine the influence of estimation errors in each linear hydrodynamic manoeuvring derivative on the results for standard manoeuvres, a sensitivity study was conducted. As stated above, similar studies have been conducted in the past for other ships and mathematical formulations. In the present study, a set of fast manoeuvres using the mathematical model above was conducted during which one of the coefficients was individually multiplied by a factor of 1.1. The forces generated by the propeller and rudder were estimated using conventional empirical

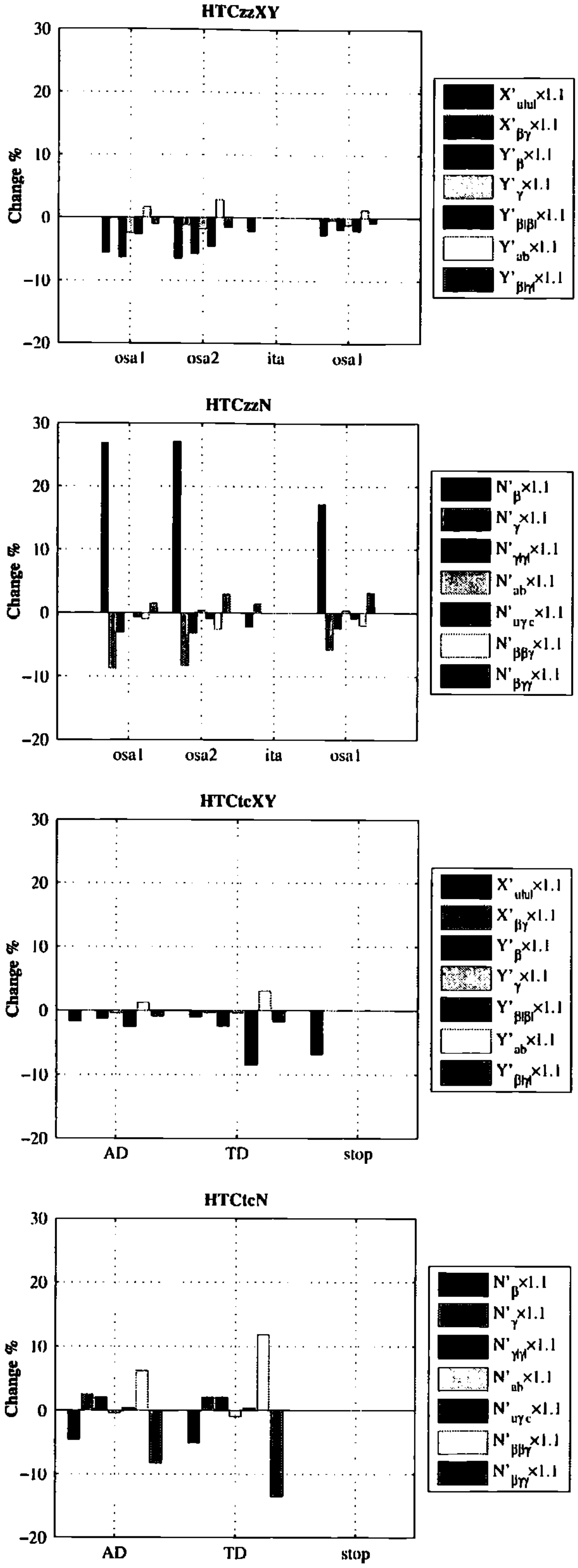

Fig. 8 Sensitivity study for HTC. *zz* zigzag, *tc* turning circle/stopping, *osa* overshoot angle, *ita* initial turning ability, *AD* advance, *TD* tactical diameter, *stop* stopping distance

Table 8 Sensitivity study, percentages, HTC

Parameter varied	10°/10° zigzag			20°/20° zigzag	35° steering angle		
	osa1	osa2	ITA	osa1	AD	TD	stop
$X'_{u\|u\|} \times 1.1$	−5.6	−6.5	−2.2	−2.6	−1.7	−1.0	−6.8
$X'_{\beta\gamma} \times 1.1$	−0.2	−1.2	0.0	−0.4	0.0	−0.3	0.0
$Y'_{\beta} \times 1.1$	−6.3	−5.7	0.0	−1.8	−1.2	−2.4	0.0
$Y'_{\gamma} \times 1.1$	−2.5	−1.9	0.0	−1.1	−0.4	−0.3	0.0
$Y'_{\beta\|\beta\|} \times 1.1$	−2.6	−4.6	0.0	−2.1	−2.5	−8.5	0.0
$Y'_{ab} \times 1.1$	1.7	2.8	0.0	1.3	1.2	3.0	0.0
$Y'_{\beta\|\gamma\|} \times 1.1$	−1.0	−1.5	0.0	−0.8	−0.8	−1.7	0.0
$N'_{\beta} \times 1.1$	26.9	27.1	−2.2	17.2	−4.6	−5.1	0.0
$N'_{\gamma} \times 1.1$	−8.7	−8.3	1.5	−5.7	2.5	2.0	0.0
$N'_{\gamma\|\gamma\|} \times 1.1$	−3.1	−3.1	0.0	−2.4	2.1	2.0	0.0
$N'_{ab} \times 1.1$	0.2	0.3	0.0	0.4	−0.4	−1.0	0.0
$N'_{u\gamma c} \times 1.1$	−0.7	−0.9	0.0	−0.8	0.4	0.3	0.0
$N'_{\beta\beta\gamma} \times 1.1$	−1.0	−2.5	0.0	−2.0	6.2	11.8	0.0
$N'_{\beta\gamma\gamma} \times 1.1$	1.5	3.0	0.0	3.1	−8.3	−13.5	0.0

osa overshoot angle, *ITA* initial turning ability, *AD* advance, *TD* tactical diameter, *stop* stopping distance

relations. Zigzag manoeuvres were conducted to obtain the first and second overshoot angles (osa) and the initial turning ability (ITA) during the 10°/10° zigzag manoeuvre and the first overshoot angle during the 20°/20° zigzag manoeuvre. From turning-circle manoeuvres with a 35° steering angle, the advance (AD) and tactical diameter (TD) were obtained. Finally, the stopping distance (stop) was calculated.

The results of the sensitivity study are shown in Fig. 8 and Table 8. It is clear that for the HTC, deviations in N'_{β} have the largest impact on the accuracy of the prediction of the yaw checking and course keeping ability; of all linear coefficients it also has the largest influence on the turning ability. N'_{γ} is also an important coefficient. Y'_{γ} is the least important linear coefficient for accurate predictions.

Furthermore, it is seen that for the zigzag manoeuvres, the linear derivatives are more important than the non-linear derivatives; during the turning circle manoeuvres, this is not the case. Also the 10°/10° zigzag manoeuvre is more sensitive to changes in the linear derivatives than the 20°/20° zigzag manoeuvre is. Similar conclusions were found by Lee and Shin [17] and Bulian et al. [18].

The sensitivity study demonstrates that for accurate predictions of manoeuvrability using coefficients derived from CFD calculations, accurate predictions of the yawing moment, in particular, must be made. It should be noted, however, that the sensitivity of the results depends on the individual ship because of different balancing between coefficients. Furthermore, other aspects, such as the efficiency of the appendages, also determine the sensitivity of the manoeuvring behaviour of the ship.

4 Conclusions

The study presented in this article demonstrates that the forces and moments acting on a ship in manoeuvring conditions can be accurately predicted using viscous flow calculations. Comparisons with empiric formulas proposed in the past show that better linear hydrodynamic derivatives can be obtained when using CFD. The CFD calculations provide the added benefit of insight into the flow around the hull. The sensitivity study demonstrates that for accurate predictions of the manoeuvrability using coefficients derived from CFD calculations, accurate predictions of the yawing moment, in particular, must be made. With the hybrid method proposed in this article, increased fidelity in manoeuvring predictions at the early design stage is expected.

Further work will concentrate on establishing hydrodynamic coefficients for the appended ship and using the coefficients in simulation programs to predict the manoeuvrability of ships. Furthermore, additional improvements in the predicted forces and moments can be expected. For this, the use of different (more advanced) turbulence models will be considered.

Acknowledgments Part of the work conducted for this article was funded by the Commission of the European Communities for the Integrated Project VIRTUE under grant 516201 in the sixth Research and Technological Development Framework Programme (Surface Transport Call).

References

1. International Maritime Organisation (2002) IMO resolution MSC. 137(76): Standards for ship manoeuvrability, International Maritime Organisation, London
2. Quadvlieg FHHA, Van Coevorden P (2003) Manoeuvring criteria: more than IMO A751 requirements alone! In: Proceedings of the MARSIM international conference on marine simulation and ship manoeuvrability, vol 2. The Society of Naval Architects of Japan and Japan Institute of Navigation, Kanazawa
3. Dand I (2003) Low-speed manoeuvring criteria: some considerations. In: Proceedings of the MARSIM international conference on marine simulation and ship manoeuvrability, vol 1. The Society of Naval Architects of Japan and Japan Institute of Navigation, Kanazawa
4. Cura Hochbaum A, Vogt M (2003) On the prediction of hydrodynamic forces on a manoeuvring ship. In: Proceedings of the MARSIM international conference on marine simulation and ship manoeuvrability, vol 3. The Society of Naval Architects of Japan and Japan Institute of Navigation, Kanazawa
5. Ohmori T (1998) A study on hydrodynamic characteristics of a maneuvering ship in shallow water by a finite-volume method. In: MAN'98 international symposium and workshop on force acting on a maneuvering vessel, Bassin d'Essais des Carènes, Val de Reuil, France
6. Jurgens AJ, Hallmann R, Tukker J (2006) Experimental investigation into the flow around a manoeuvring LNG carrier on shallow water. In: Proceedings of the NAV international conference on ship and shipping research, Cetena, Genova
7. Hino T (ed) (2005) Proceedings of the CFD workshop, National Maritime Research Institute, Tokyo
8. Hoekstra M (1999) Numerical simulation of ship stern flows with a space-marching Navier–Stokes method. PhD thesis, Faculty of Mechanical Engineering and Marine Technology, Delft University of Technology
9. Raven HC, van der Ploeg A, Eça L (2006) Extending the benefit of CFD tools in ship design and performance prediction. In: Proceedings of the seventh ICHD international conference on hydrodynamics, University of Naples "Federico II", Ischia, pp 573–580
10. Menter FR (1997) Eddy viscosity transport equations and their relation to the k–ε model. J Fluid Eng 119:876–884
11. Dacles-Mariani J, Zilliac GG, Chow JS, Bradshaw P (1995) Numerical/experimental study of a wing tip vortex in the near field. AIAA J 33:1561–1568
12. Eça L, Hoekstra M, Windt J (2002) Practical grid generation tools with applications to ship hydrodynamics. In: Proceedings of the eighth international conference on grid generation in computational field simulations
13. Toxopeus SL (2005) Verification and validation of calculations of the viscous flow around KVLCC2M in oblique motion. In: Proceedings of the fifth Osaka colloquium, Osaka Prefecture University, Osaka, pp 200–209
14. Toxopeus SL (2006) Calculation of hydrodynamic manoeuvring coefficients using viscous-flow calculations. In: Proceedings of the seventh ICHD international conference on hydrodynamics, University of Naples "Federico II", Ischia, pp 493–502
15. Vassalos D, Park SH, Lee BS (1995) Developing a manoeuvring design capability for naval vessels. In: Proceedings of the PRADS practical design of ships and other floating bodies conference, Seoul, pp 1.616–1.617
16. Ishiguro T, Tanaka S, Yoshimura Y (1996) A study on the accuracy of the recent prediction technique of ship's manoeuvrability at the early design stage. In: Proceedings of the MARSIM international conference on marine simulation and ship manoeuvring, Danish Maritime Institute, Copenhagen, pp 547–561
17. Lee H-Y, Shin S-S (1998) The prediction of ship's manoeuvring performance in the initial design stage. In: Proceedings of the PRADS practical design of ships and other floating bodies conference, Maritime Research Institute Netherlands, The Hague, pp 633–639
18. Bulian G, Nicolosi RG, Francescutto A (2006) On the effect of uncertainty modeling in the hydrodynamic derivatives of a ship manoeuvring mathematical model. In: Proceedings of the seventh ICHD international conference on hydrodynamics, University of Naples "Federico II", Ischia, pp 359–368
19. Clarke D, Gedling P, Hine G (1983) The application of manoeuvring criteria in hull design using linear theory. Trans RINA 125:45–68
20. Hooft JP, Pieffers JBM (1988) Maneuverability of frigates in waves. Mar Technol 25(4):262–271
21. Hooft JP (1994) The cross flow drag on a manoeuvring ship. Ocean Eng 21(3):329–342
22. Kume K, Hasegawa J, Tsukada Y et al (2006) Measurements of hydrodynamic forces, surface pressure, and wake for obliquely towed tanker model and uncertainty analysis for CFD validation. J Mar Sci Technol 11:65–75
23. Kijima K, Nakiri Y, Furukawa Y (2000) On a prediction method for ship manoeuvrability. In: Proceedings of the international workshop on ship manoeuvrability-25 years CPMC at HSVA, Hamburg
24. Toxopeus SL (2006) Validation of slender-body method for prediction of linear manoeuvring coefficients using experiments and viscous-flow calculations. In: Proceedings of the seventh ICHD international conference on hydrodynamics, University of Naples "Federico II", Ischia, pp 589–598